

Heteroreceptor Complexes Formed by Dopamine D₁, Histamine H₃, and N-Methyl-D-Aspartate Glutamate Receptors as Targets to Prevent Neuronal Death in Alzheimer's Disease

Mar Rodríguez-Ruiz^{1,2}

Estefanía Moreno^{1,2}

David Moreno-Delgado^{1,2}

Gemma Navarro^{1,2}

Josefa Mallol^{1,2}

Antonio Cortés^{1,2}

Carme Lluís^{1,2}

Enric I. Canela^{1,2}

Vicent Casadó^{1,2}

Peter J. McCormick^{1,2,3}

Rafael Franco^{1,2,4,*}

Phone +34 934021208

Email rfranco@ub.edu

Email rfranco123@gmail.com

¹ Molecular Neurobiology laboratory, Department of Biochemistry and Molecular Biology, University of Barcelona, Barcelona, Spain

² Centro de Investigación en Red, Enfermedades Neurodegenerativas

(CIBERNED), Instituto de Salud Carlos III, Madrid, Spain

³ Present Address: School of Pharmacy, University of East Anglia, Norwich Research Park, Norwich, NR4 7TJ UK

⁴ Departament de Bioquímica i Biologia Molecular, Facultat de Biologia, Universitat de Barcelona, Diagonal 643, Prevesti Building, 08028 Barcelona, Spain

Abstract

Alzheimer's disease (AD) is a neurodegenerative disorder causing progressive memory loss and cognitive dysfunction. Anti-AD strategies targeting cell receptors consider them as isolated units. However, many cell surface receptors cooperate and physically contact each other forming complexes having different biochemical properties than individual receptors. We here report the discovery of dopamine D₁, histamine H₃, and N-methyl-D-aspartate (NMDA) glutamate receptor heteromers in heterologous systems and in rodent brain cortex. Heteromers were detected by co-immunoprecipitation and in situ proximity ligation assays (PLA) in the rat cortex where H₃ receptor agonists, via negative cross-talk, and H₃ receptor antagonists, via cross-antagonism, decreased D₁ receptor agonist signaling determined by ERK1/2 or Akt phosphorylation and counteracted D₁ receptor-mediated excitotoxic cell death. Both D₁ and H₃ receptor antagonists also counteracted NMDA toxicity suggesting a complex interaction between NMDA receptors and D₁-H₃ receptor heteromer function. Likely due to heteromerization, H₃ receptors act as allosteric regulator for D₁ and NMDA receptors. By bioluminescence resonance energy transfer (BRET), we demonstrated that D₁ or H₃ receptors form heteromers with NR1A/NR2B NMDA receptor subunits. D₁-H₃-NMDA receptor complexes were confirmed by BRET combined with fluorescence complementation. The endogenous expression of complexes in mouse cortex was determined by PLA and similar expression was observed in wild-type and APP/PS1 mice. Consistent with allosteric receptor-receptor interactions within the complex, H₃ receptor antagonists reduced NMDA or D₁ receptor-mediated excitotoxic cell death in cortical organotypic cultures. Moreover, H₃ receptor antagonists reverted the

toxicity induced by β_{1-42} -amyloid peptide. Thus, histamine H_3 receptors in D_1 - H_3 -NMDA heteroreceptor complexes arise as promising targets to prevent neurodegeneration.

Keywords

Alzheimer's disease
Dementia
G-protein-coupled receptors
Heteroreceptor complexes
Ionotropic receptor
Neuroprotection
Receptor heteromers

Mar Rodríguez-Ruiz, Estefanía Moreno, David Moreno-Delgado, Vicent Casadó, Peter J. McCormick and Rafael Franco contributed equally to this work.

Electronic supplementary material

The online version of this article (doi: 10.1007/s12035-016-9995-y) contains supplementary material, which is available to authorized users.

Introduction

Current Alzheimer's disease (AD) therapies mainly target acetyl cholinesterase to enhance cholinergic neurotransmission. However, neurodegeneration is not limited to a specific neurotransmitter system. Glutamatergic, serotonergic, adrenergic, dopaminergic, and peptidergic neurotransmitter systems are also deregulated in AD [1]. Impaired neuronal signaling may affect amyloid precursor protein (APP) proteolysis and promote amyloid formation in the AD brain. In addition, amyloid toxicity and neurodegeneration may affect neurotransmission, suggesting the involvement of complex positive-feedback loops in the pathogenesis of the disease. Consequently, a complementary approach that includes modulation of neurotransmission in addition to lowering the amyloid burden is an attractive therapeutic strategy for the treatment of AD [1–3]. Indeed, activation of dopamine D_1 -like receptors protects neurons from

synapse dysfunction induced by amyloid oligomers [4] and we and others have shown that dopamine facilitates hippocampal acetyl-choline release by acting on D₁-like receptors that are G protein-coupled receptors (GPCR) located in hippocampal cholinergic terminals [5–8]. Moreover, activation of dopamine D₁ receptors (D₁R) enables working memory by enhancing the firing of pyramidal neurons [9, 10]. Thus, the dopaminergic system is a key neurotransmitter system involved in AD. Another key neurotransmitter system implicated in AD is the histaminergic system [11–15] and GPCR histamine 3 receptors (H₃R) are widely expressed in the CNS, particularly in the frontal cortex and hippocampus [16]. H₃R antagonists are promising drugs for AD [17–19] but the exact mode of action is more complex than suspected. One potential mechanism may be the blockade of histamine receptors in a specific CNS hetero-oligomeric context. Indeed, hetero-oligomerization of proteins is a recurrent phenomenon in biology [20, 21]. Dopamine D₁ GPCRs interact in striatum with inter alia the histamine H₃ receptor. Whereas D₁ receptors are coupled to heterotrimeric G_s proteins and histamine H₃ receptors couple to G_i/G_o, D₁/H₃ receptor heteromers (D₁/H₃RHets) allow histamine H₃ receptor agonists to activate the mitogen-activated protein kinase (MAPK) pathway. The link between histamine receptors and MAPK depends on heteromer formation as it does not happen in D₁ receptor-deficient mice [6, 22].

In the case of ionotropic glutamate receptors, formation of hetero-oligomers is needed for proper function. In transfected cells, N-methyl-D-aspartate (NMDA) regulates dopamine D₁ receptor trafficking and desensitization by a direct interaction between the ionotropic glutamate (NMDA) and the metabotropic dopamine (D₁) receptors [23]. Lee et al. (2002) showed, also in an heterologous system, that the cytoplasmic tail of the D₁ receptor has two epitopes to interact with NR1-1a and NR2A subunits of the NMDA receptor [24, 25]. The interaction with NR1-1a affects NMDA receptor-mediated excitotoxicity while the interaction with NR2A affects ligand-gated currents. Besides inhibitors of acetyl cholinesterase, the only drug approved for Alzheimer's disease is Namenda^R whose active component, memantine, is an allosteric modulator of NMDA receptors [26], which remain one of the main therapeutic targets in this neurodegenerative disease [27]. As heteroreceptor complexes formed by different GPCRs [28] or by combination of GPCR and ionotropic receptors [29] have specific physiological functions and emerge as novel therapeutic

targets, the aim of the present paper was to look for heteromers formed by dopamine D₁, histamine H₃, and NMDA receptors and to assess their potential as targets in Alzheimer's disease.

Materials and Methods

Animals

Two-month-old male Sprague Dawley rats (animal facility of the Faculty of Biology, University of Barcelona) were housed two per cage and kept on a 12/12-h dark/light cycle with food and water available ad libitum and experiments were performed during the light cycle. Animals were anesthetized with 4 % isoflurane and euthanized by decapitation. APP/PS1 mice and wild-type (WT) littermates were used. The generation of mice expressing the human mutated forms of the amyloid precursor protein (APP^{swe}) and presenilin-1 (PS1^{dE9}) is described elsewhere [3]. In the present study, identification of transgenic mice was carried out as follows: genomic DNA was isolated from 1-cm tail clips and genotyped by polymerase chain reaction (PCR) technique using the PCR conditions proposed by the Jackson Laboratory (www.jax.org). Animals were maintained under standard animal housing conditions in a 12-h dark–light cycle with free access to food and water. Animal procedures were conducted according to ethical guidelines (European Communities Council Directive 2010/63/EU) and approved by the animal experimentation ethics committee of the Catalan Government (CEEA-DAAM 6419 and CEEA/DMAH 4049 and 5664).

Co-Immunoprecipitation Experiments

Rat cortical tissue was homogenized at 4 °C in 50 mM Tris–HCl buffer, pH 7.4, containing a protease inhibitor mixture (1/1000, Sigma-Aldrich, St. Louis, MO, USA) using a Polytron homogenizer, and membranes were obtained by centrifugation at 105,000g for 1 h at 4 °C. Membranes were washed three more times at the same conditions and were solubilized by homogenization in ice-cold immunoprecipitation buffer (phosphate-buffered saline, pH 7.4, containing 1 % (v/v) Nonidet P-40) and incubated for 30 min on ice before centrifugation at 105,000g for 1 h at 4 °C. Using a Dynabeads® Protein G kit (Invitrogen, Paisley, Scotland, UK), the supernatant (1 mg/ml of protein) was processed as described in the immunoprecipitation protocol. Protein content was quantified

by the bicinchoninic acid method (Pierce) using bovine serum albumin dilutions as standard. Immunoprecipitation was carried out with a rat anti-D₁ receptor antibody (1:1000, Sigma-Aldrich). As negative control, anti-calnexin antibody was used (1:1000, BD Biosciences Pharmingen, San Diego, CA, USA). Immunoprecipitates were separated on a denaturing 10 % SDS-polyacrylamide gel and transferred onto PVDF membranes to perform western blot assays. Membranes were probed with guinea pig anti-D₁ receptor (1:1000, Frontier Institute, Ishikari, Hokkaido, Japan) and rabbit anti-H₃ receptor (1:1000, Alpha diagnostic, San Antonio, Texas, USA) antibodies and the appropriate secondary antibodies: goat anti-guinea pig-peroxidase (1:20,000, Sigma-Aldrich) and goat anti-rabbit-peroxidase (1:20,000, Thermo Scientific, Fremont, CA). Bands were visualized with a LAS-3000 equipment (Fujifilm). Data analysis was performed by Image Gauge software (version 4.0) and Multi Gauge software (version 3.0).

Preparation of Rat and Mouse Brain Sections and Slices

For PLA experiments, rat and mouse brains were rapidly removed and fixed with 4 % paraformaldehyde solution for 24 h at 4 °C. Brains were then washed in PBS, cryo-preserved in a 30 % sucrose solution for 48 h at 4 °C, and stored at -20 °C until sectioning. Cortical 15- μ m thick sections were cut on a freezing cryostat (Leica Jung CM-3000, Leica Microsystems, Mannheim, Germany) and mounted on glass slides. For cell death determination and signaling experiments, the brains were rapidly removed and placed in ice-cold oxygenated (O₂/CO₂: 95/5 %) Krebs-bicarbonate buffer (in millimolars: 124 NaCl, 4 KCl, 1.25 KH₂PO₄, 1.5 MgCl₂, 1.5 CaCl₂, 10 glucose, and 26 NaHCO₃) pH 7.4. The brains were sliced along the coronal plane at 4 °C using a brain matrix (Zivic Instruments, Pittsburgh, PA, USA). Cortical slices (500 μ m thick) were kept at 4 °C in Krebs-bicarbonate buffer during the dissection.

Cell Culture, Expression Vectors and Transient Transfection

Human embryonic kidney (HEK-293 T) cells were grown in Dulbecco's modified Eagle's medium (DMEM) supplemented with 2 mM L-glutamine, 100 μ g/ml sodium pyruvate, 100 units/milliliter penicillin/streptomycin, MEM non-essential amino acid solution (1/100), and 5 % (v/v) heat-inactivated fetal

bovine serum (FBS) (all supplements were from Invitrogen). For transfection, sequences encoding receptors or fusion proteins consisting of the human receptors fused to *Renilla luciferase* (Rluc) or to yellow fluorescent protein (YFP) on the C-terminal end of the receptor (D₁R-YFP, H₃R-YFP, CB₁R-Rluc), of human (H₃, D₁, and CB₁) receptors fused to the YFP Venus N-terminal fragment (n-YFP), or of human (serotonin 5-HT_{2B}, H₃, and D₁) fused to the YFP Venus C-terminal fragment (c-YFP) were obtained and characterized as previously described (Navarro et al. 2008; [6, 7, 31, 32]).

Plasmids encoding human NR1A-Rluc and NR2B were generously provided by Dr. Julie Perroy from the University of Montpellier (France). HEK-293 T cells growing in 35-mm diameter six-well plates were transiently transfected with cDNAs by the ramified polyethylenimine (PEI; Sigma-Aldrich) method. Cells were incubated (4 h) with cDNAs, ramified PEI (5 ml/mg cDNA of 10 mM PEI) and 150 mM NaCl in a serum-free medium. After 4 h, the medium was changed to a fresh complete culture medium. Forty-eight hours after transfection, cells were washed twice in quick succession in HBSS containing the following (in millimolars): 137 NaCl, 5 KCl, 0.34 Na₂HPO₄ × 12 H₂O, 0.44 KH₂PO₄, 1.26 CaCl₂ × 2 H₂O, 0.4 MgSO₄ heptahydrate, 0.5 MgCl₂, 10 HEPES, pH 7.4, supplemented with 0.1 % glucose (w/v), detached by gently pipetting, and resuspended in the same buffer. To control the cell number, sample protein concentration was determined using a Bradford assay kit (Bio-Rad) using bovine serum albumin (BSA) dilutions as standards. HEK-293 T cell suspension (20 µg of protein) was distributed into 96-well microplates; black plates with a transparent bottom (Porvair, King's Lynn, UK) were used for fluorescence determinations, whereas white opaque plates (Sigma-Aldrich) were used for bioluminescence resonance energy transfer (BRET) experiments.

Fluorescence Complementation Assays

HEK-293 T cells were transiently co-transfected with the cDNA encoding for H₃, D₁, or CB₁ receptors fused to the YFP Venus N-terminal fragment (n-YFP) and 5-HT_{2B}, H₃, or D₁ receptors fused to the YFP Venus C-terminal fragment (c-YFP). To quantify the amount of reconstituted YFP Venus, cells (20 µg protein) were distributed in 96-well plates (black plates with a transparent bottom, Porvair), and emission fluorescence at 530 nm was read in a FluoStar Optima plate fluorometer (BMG Labtechnologies, Ortenberg, Germany)

equipped with a high-energy xenon flash lamp, using a 10-nm bandwidth excitation filter at a 400-nm reading. Protein fluorescence expression was determined as fluorescence of the sample minus the fluorescence of cells not expressing the fusion proteins (basal). Cells expressing two receptor-cYFP or two receptor-nYFP fusion proteins showed similar fluorescence levels to non-transfected cells.

BRET and BRET with Bimolecular Fluorescence Complementation

HEK293 T cells were transiently co-transfected with a constant amount of cDNA encoding for the receptor fused to Rluc and with increasing amounts of cDNA for the receptor fused to YFP (see figure legends). To quantify receptor-YFP expression, fluorescence of cells (20 μ g protein) was read in a FluoStar Optima Microplate Fluorometer (BMG Labtechnologies) equipped with a high-energy xenon flash lamp, using a 10-nm bandwidth excitation filter at 400 nm reading. For bioluminescent resonance energy transfer (BRET) or BRET with bimolecular fluorescence complementation (BiFC) measurements, 5 μ M coelenterazine H (Invitrogen) was added to the equivalent of 20 μ g of cell suspension. After adding coelenterazine H (1 min for BRET or 5 min for BRET with BiFC), readings were collected using a Mithras LB 940 that allows the integration of the signals detected in the short-wavelength filter at 485 nm (440–500 nm) and the long-wavelength filter at 530 nm (510–590 nm). To quantify receptor-Rluc expression, luminescence readings were also performed after 10 min of adding 5 μ M coelenterazine H. The net BRET is defined as $[(\text{long-wavelength emission})/(\text{short-wavelength emission})] - \text{cf.}$, where cf. corresponds to $[(\text{long-wavelength emission})/(\text{short-wavelength emission})]$ for the donor construct expressed alone in the same experiment. Data were fitted to a nonlinear regression equation, assuming a single-phase saturation curve with GraphPad Prism software. BRET is expressed as milliBRET units (mBU).

Determination of Phospho-Extracellular-Signal Regulated Kinase (ERK1/2) and Phospho-Akt/Protein Kinase B (PKB)

After dissection, fresh cortical slices were transferred into 1 ml of ice-cold Krebs-bicarbonate buffer. The temperature was raised to 23 °C and after 30 min, the culture medium was replaced by 2 ml of fresh Krebs-bicarbonate buffer (23 °C). Slices were incubated under constant oxygenation (O_2/CO_2 :

95 %/5 %) at 30 °C for 4–5 h in an Eppendorf thermomixer (5 Prime, Inc., Boulder, CO, USA). The medium was replaced by 200 µl of fresh Krebs-bicarbonate buffer and incubated for 30 min before the addition of any agent. Slices were treated with the indicated ligand concentration for the indicated time and lysed with (in millimolars) 50 Tris–HCl pH 7.4, 50 NaF, 150 NaCl, 45 mM glycerol-3-phosphate, 0.02 phenyl-arsine oxide, 0.4 NaVO₄, and 1 % Triton X-100 and protease inhibitor cocktail. Cellular debris was removed by centrifugation at 13,000g for 10 min at 4 °C and total protein was quantified by the bicinchoninic acid method using bovine serum albumin dilutions as standard. To determine the degree of protein phosphorylation, equivalent amounts of protein were separated by electrophoresis on a denaturing 10 % SDS-polyacrylamide gel and transferred onto PVDF-FL membranes. Odyssey blocking buffer (LI-COR Biosciences, Lincoln, NE, USA) was then added, and the membrane was rocked for 90 min. The membranes were then probed overnight with a mixture of a mouse anti-phospho-ERK1/2 antibody (1:2500; Sigma-Aldrich), a rabbit anti-phospho-Ser473-Akt antibody (1/2500, SAB Signalway Antibody, Pearland, Texas, USA), and a rabbit anti-ERK1/2 antibody that recognizes both phosphorylated and unphosphorylated ERK1/2 (1:40,000; Sigma-Aldrich). The 42- and 44-kDa bands corresponding to ERK1 and ERK2 were visualized by the addition of a mixture of IRDye 800 (anti-mouse) antibody (1:10,000; Sigma-Aldrich) and IRDye 680 (anti-rabbit) antibody (1:10,000; Sigma-Aldrich) for 2 h and scanned by the Odyssey infrared scanner (LI-COR Biosciences). Band densities were quantified using the scanner software and exported to Excel (Microsoft, Redmond, WA, USA). The level of phosphorylated ERK1/2 isoforms or of pAkt/PKB was normalized for differences in loading using the total ERK1/2 protein band intensities.

Cell Death Determination in Rat and Mouse Organotypic Cultures

Immediately after dissection, brain slices (500 µm thickness, see above) were placed in six-well plates containing Millicell-CM organotypic tissue culture plate inserts (EMD Millipore Corporation, Billerica, MA, USA) and cultured at 37 °C with Neurobasal medium supplemented with 20 % horse serum, 0.5 % B27, 2 mM L-glutamine, 100 µg/ml sodium pyruvate, MEM non-essential amino acid solution (1/100), and 100 units/milliliter penicillin/streptomycin (all supplements were from Invitrogen). After 24 h, culture medium was replaced

by fresh medium containing no ligands or the indicated concentrations of SKF-81297, SCH-23390, NMDA, MK-801, or thioperamide 1 h before the addition of the excitotoxic agents (D_1 or NMDA receptor agonists at 50 μM). Slices were maintained 48 h more in culture and, after a total 72 h of incubation, 10 μM propidium iodide (PI) was added to culture medium, which was maintained at 37 °C for 1 h. Slices were then removed from the incubator, washed twice in cold-PBS and fixed with 4 % paraformaldehyde for 1 h at 4 °C. Nuclei were stained with 1:1000 Hoechst for 1 h. Total (Hoechst-stained) and PI-positive nuclei were quantified to evaluate cell death using Leica SP2 confocal microscope (20 \times ; UV, 561 lasers) and the quantification program Image-based Tool for Counting Nuclei for ImageJ.

In Situ Proximity Ligation Assays (PLA)

Rat or mouse cortical brain sections were mounted on glass slides, thawed at 4 °C, washed in 50 mM Tris-HCl, 0.9 % NaCl pH 7.8 buffer (TBS), permeabilized with TBS containing 0.01 % Triton X-100 for 10 min, and repeatedly washed with TBS. Heteromers were detected using the Duolink II in situ proximity ligation assays (PLA) detection Kit (Sigma-Aldrich) following the instructions of the supplier. To detect D_1 - H_3 , NMDA/NR1- D_1 , or NMDA/NR1- H_3 heteroreceptor complexes, we used a mixture of equal amounts of the following pairs of primary antibodies: (i) guinea pig anti- D_1 receptor (Frontier Institute, Hokkaido, Japan) and rabbit anti- H_3 (Alpha diagnostic) receptors, (ii) guinea pig anti- D_1 and rabbit anti-NMDA/NR1 (Abcam Inc., Cambridge, MA, USA) antibodies, or (iii) rabbit anti-NMDA/NR1 antibody directly coupled to a *minus* DNA chain and rabbit anti- H_3 receptor antibody directly coupled to a *plus* DNA chain (obtained following the instructions of the Sigma-Aldrich supplier). PLA probes detecting guinea pig or rabbit antibodies were used to detect D_1 - H_3 and NMDA/NR1- D_1 receptor complexes. Then samples were processed for ligation and amplification and were mounted using a DAPI-containing mounting medium. Samples were observed in a Leica SP2 confocal microscope equipped with an apochromatic 63X oil-immersion objective (N.A. 1.4), and a 405-nm and a 561-nm laser lines. For each field of view a stack of two channels (one per staining) and six to seven Z stacks with a step size of 1 μm were acquired. Quantification of cells containing one or more red spots versus total cells (blue nucleus) and, in cells containing spots, the

ratio r (number of red spots/cell) were determined, using the Fiji package (<http://pacific.mpi-cbg.de/>), considering a total 1000–2000 cells from 7 to 16 different fields from three different animals. Nuclei and red spots were counted on the maximum projections of each image stack. After getting the projection each channel was processed individually. The nuclei were segmented by filtering with a median filter, subtracting the background, enhancing the contrast with the Contrast Limited Adaptive Histogram Equalization (CLAHE) plug-in, and finally applying a threshold to obtain the binary image and the regions of interest (ROI) around each nucleus. Red spot images were also filtered and thresholded to obtain the binary images. Red spots were counted in each of the ROIs obtained in the nuclei images. The number of red dots after PLA was negligible in the negative controls constituted by sections only incubated with one primary antibody (anti-D₁R in rat and mouse slices and anti-H₃R in mouse slices).

Statistical Analysis

The data in the graphs are presented as the mean \pm SEM. Statistical analysis was performed with SPSS 18.0 software. The test of Kolmogorov–Smirnov with the correction of Lilliefors was used to evaluate the fit of the data to a normal distribution and the test of Levene to evaluate the homogeneity of variance. Significance was analyzed by two-way or one-way ANOVA followed by post hoc test (see figure legends) for multiple comparisons. Significant differences were considered when $p < 0.05$.

Results

Identification of Heteromers in Brain Cortex

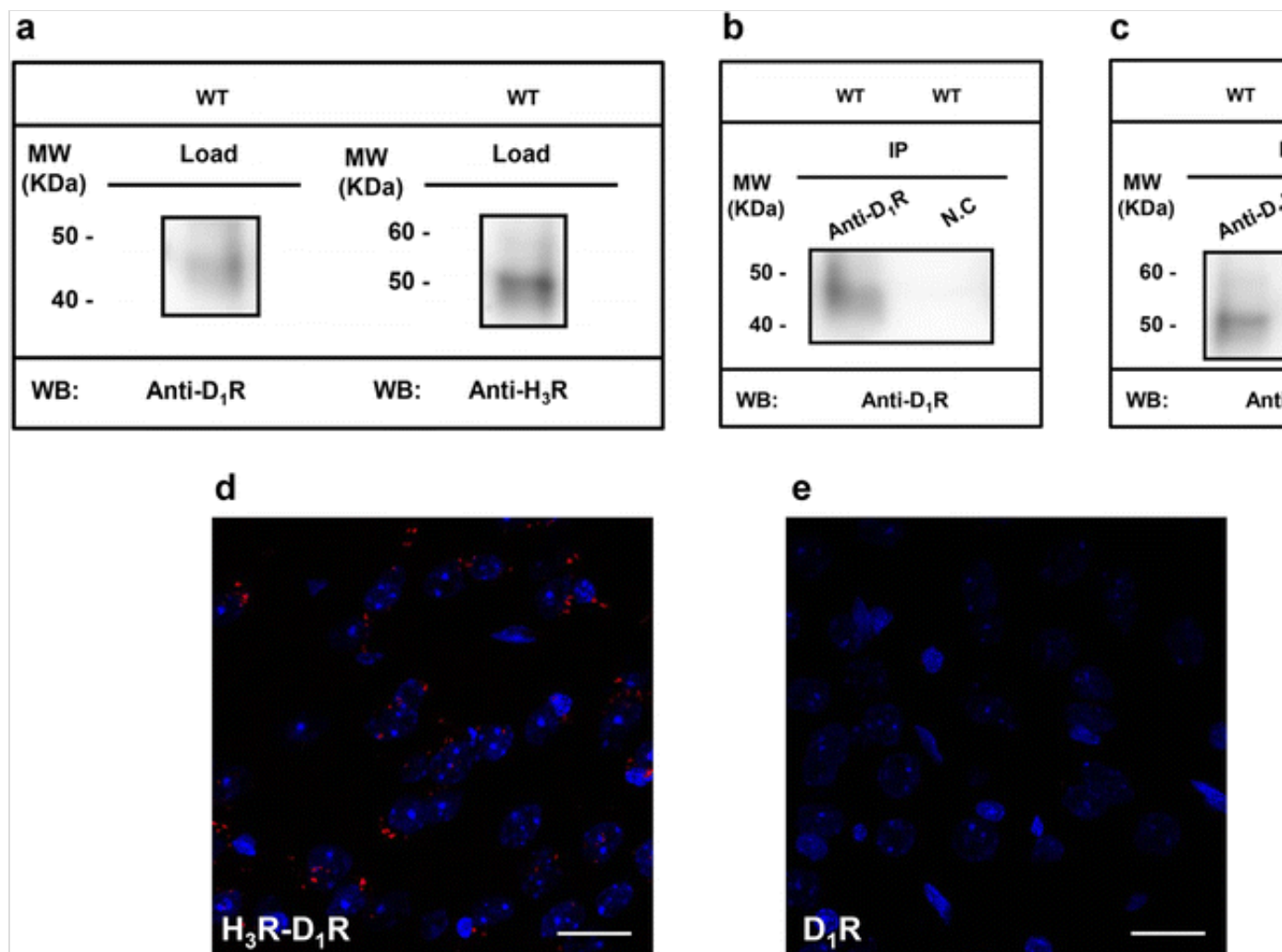
D₁/H₃ heteroreceptor complexes (D₁/H₃RHets) have been described in the striatum [22]. In an attempt to identify D₁/H₃RHets in the cerebral cortex, co-immunoprecipitation and in situ proximity ligation assays (PLA) were performed in rat samples. Detergent extracts from rat cortex were immunoprecipitated with antibodies against D₁ receptors and immunoblotted using either anti-D₁ or anti H₃-receptor antibodies. Results depicted in Fig. 1a–c indicate that immunoprecipitates contained both receptors. The in situ proximity ligation assay (PLA), which allows detection of proteins in close

proximity, confirmed in cortical sections that D₁ and H₃ receptors form aggregates, detected as red dots in some of the neural cells (Fig. 1d). The number of red dots after PLA was negligible in the negative controls constituted by sections only incubated with one primary antibody (anti-D₁ receptor antibody; Fig. 1e).

Fig. 1

Detection of D₁-H₃ receptor heteromers in samples from rat cortex. Co-immunoprecipitation experiments (a–c) and PLA (d, e) were performed in samples from rat cortex. Solubilized rat cortical membranes (a) and immunoprecipitates with anti-D₁ receptor or anti-calnexin antibodies as negative control (NC) (b, c) were analyzed by SDS-PAGE and immunoblotted using anti-D₁ or anti-H₃ receptor antibodies. *IP* immunoprecipitation, *WB* western blotting, *MW* molecular weight. PLA experiments were performed as indicated in “Materials and Methods” and D₁/H₃ receptor complexes (d) were visualized as red spots around blue-colored DAPI-stained nucleus; the negative control (e) was performed in sections incubated with one primary antibody (against the D₁ receptor). Scale bar: 20 μm

AQ1



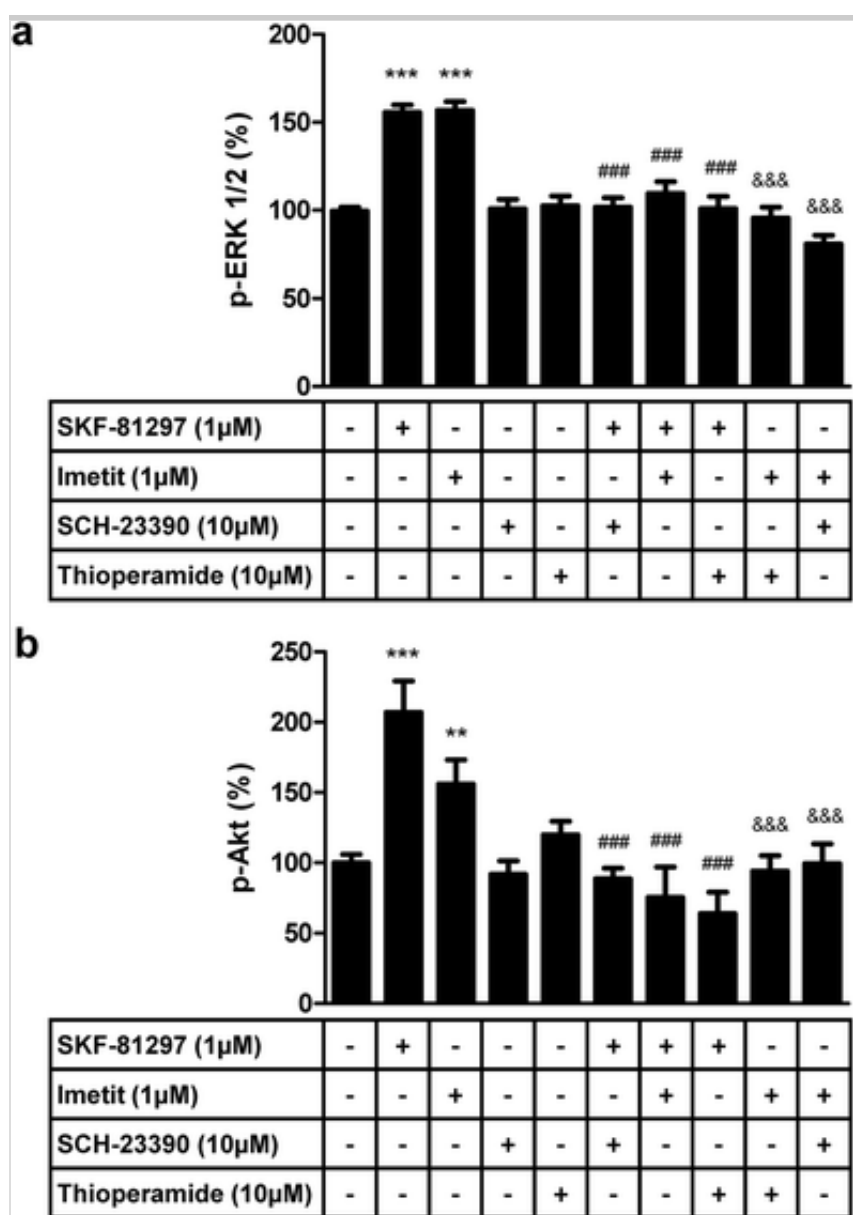
As previously reported, D₁/H₃RHets may couple to the MAP kinase pathway [22]. Slices from rat cortex were incubated (8 min) with agonists, and ERK1/2 and Akt phosphorylation were assayed. Activation of D₁ or H₃ receptors using, respectively, 1 μ M SKF-81297 or 1 μ M imetit, led to significant ERK1/2 phosphorylation that was blocked by their respective selective antagonists (10 μ M SCH-23390 or thioperamide). Interestingly, the antagonist of D₁ receptors blocked the effect of H₃ receptor agonists and the antagonist of H₃ receptors blocked the effect of D₁ receptor agonists (Fig. 2a). Fairly similar results were obtained on analyzing pAkt data (Fig. 2b). Such cross-antagonism is a common feature of receptor heteromers that may be considered as a D₁/H₃RHet print.

Fig. 2

a, b Signaling cross-talk and cross-antagonism on ERK 1/2 and Akt phosphorylation in rat cortical slices. Slices were preincubated with Krebs-bicarbonate buffer or antagonists (10 μ M thioperamide or 10 μ M SCH-23390) for

20 min prior to the addition of agonists (1 μ M SKF-81297), followed by a further incubation of 10 min. ERK1/2 or Akt phosphorylation was determined as described in “Materials and Methods.” For each treatment, the immunoreactive bands from eight slices obtained in two different experiments from a total of ten animals were quantified, and values represent the mean \pm SEM of the percentage of phosphorylation relative to basal levels found in untreated slices (100 %). Significant differences were calculated by one-way ANOVA with post hoc Bonferroni’s test for multiple comparisons ($***p < 0.001$ compared with the control condition; $###p < 0.001$ compared with SKF-81297 treatment; $&&&p < 0.001$ compared with imetit treatment)

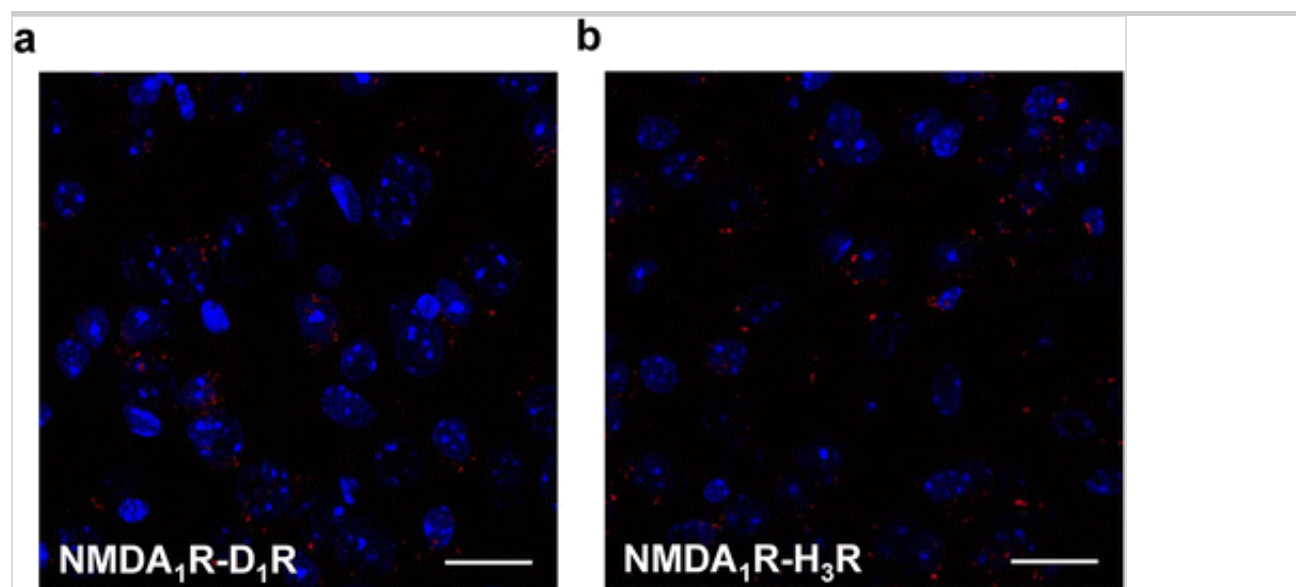
AQ2



Since previous reports from different laboratories [23, 24] have described the *in vitro* interaction between the NR1A subunit of NMDA receptor and D₁ receptors, we investigated by PLA whether aggregates formed by NMDA and D₁ receptors or NMDA and H₃ receptors could be detected in sections from rat cortex. PLA experiments were performed in rat cortical sections using antibodies specific for the two GPCRs and for the NR1A subunit. PLA data indicated the existence of NR1A-D₁ or NR1A-H₃ receptors in close proximity (Fig. 3a, b). Very few red dots were found in negative controls performed with primary antibodies against D₁, Fig. 1e, or against H₃ receptors (not shown). Overall, these results indicate that the three proteins, D₁, H₃, and NMDA glutamate receptors, may be as close as to form heteromeric complexes in the brain cortex.

Fig. 3

Detection of NR1-D₁ and NR1-H₃ receptor complexes in rat cortex. PLA experiments were performed in rat cortical sections as indicated in “Materials and Methods.” NMDA/NR1A-D₁ (a) and NMDA/NR1A-H₃ (b) receptor complexes were visualized as red spots around blue-colored DAPI-stained nucleus. Scale bar: 20 μm



In Vitro Identification of Heteromers Formed by D₁, H₃, and NMDA Receptors

The next aim was to establish whether D₁, H₃, and NMDA receptors could form

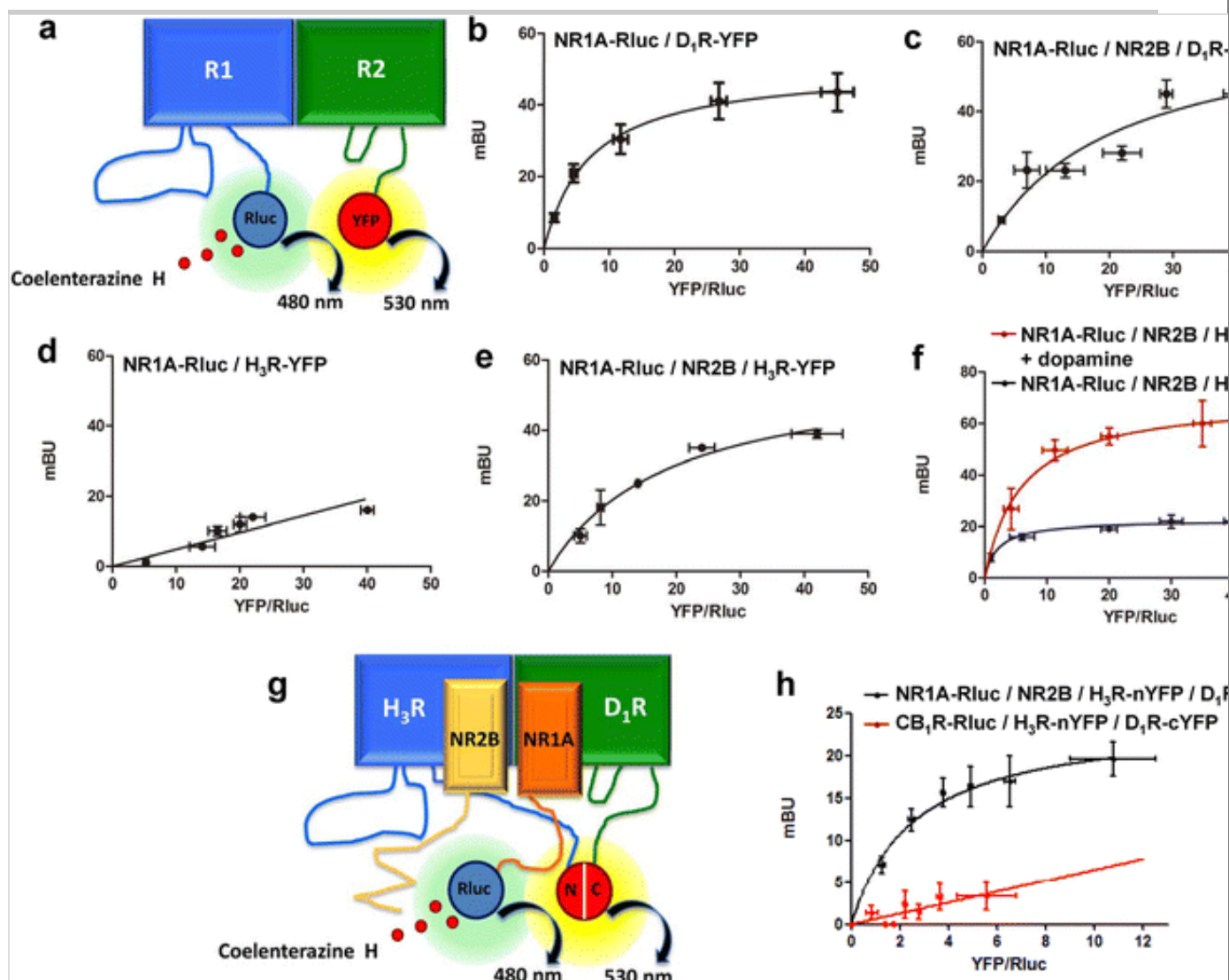
heteromeric complexes in heterologous cells expressing the three receptors. To attempt to identify the formation of direct interactions involving these receptors, a combination of bioluminescence resonance energy transfer (BRET) and bimolecular fluorescence complementation (BiFC) was undertaken. HEK-293 T cells were transfected with cDNAs encoding for fusion proteins formed by Rluc or YFP and the whole open reading frame of D₁, H₃, or the NR1A subunit of NMDA receptors. Cells expressing the NR1A subunit fused to Rluc and D₁R-YFP provided a saturable BRET signal that proves the interaction between the two proteins (Fig. 4b). BRET₅₀ was 7.0 ± 0.7 mBU and BRET_{max} was 51 ± 2 mBU (mean ± SD; *n* = 3–6). As the NR2B subunit is needed for surface expression of NMDA receptors, the experiment was repeated in cells expressing NR1A and NR2B subunits. BRET signal was saturable indicating that NR1A-Rluc does interact with D₁-YFP even in the presence of the third protein (Fig. 4c). BRET₅₀ was 20 ± 10 mBU and BRET_{max} was 70 ± 20 mBU (mean ± SD; *n* = 3–6). Different BRET₅₀ values in the absence and presence of NR2B subunit indicate that the hetero-oligomer forms with a different affinity. BRET data using H₃ and NMDA receptors were qualitatively different. On the one hand, the NR1A-Rluc subunit did not provide specific BRET readouts when transfected with H₃-YFP receptors, i.e., the relationship with the acceptor/donor ratio was linear, thus showing a lack of interaction (Fig. 4d). On the other hand, BRET between NR1A-Rluc and H₃-YFP converted into saturable when the NR2B subunit was co-expressed (Fig. 4e). Taken together, data indicate that H₃ and D₁ receptors may form a complex with functional NR1A/NR2B NMDA receptors. Importantly, evidence for complexes having the three receptors was obtained by the dopamine-induced increase of BRET_{max} between NR1A-Rluc and H₃-YFP (in the presence of D₁ and NR2B) (Fig. 4f). To know whether a macromolecular complex may include the four proteins, a BRET with bimolecular fluorescence complementation assay was performed. For complementation experiments, different ratios of plasmids encoding fusion proteins constituted by H₃ or D₁ receptors and one half of the YFP (H₃R-nYFP and D₁R-cYFP) were assayed to optimize fluorescence emission after complementation (ESM 1: Fig. S1a, b). The optimal cDNA ratio was 1.5 and 4 µg for, respectively, plasmids coding H₃R-nYFP or D₁R-cYFP or (ESM 1: Fig. S1). The assayed negative controls were those constituted by non interacting pairs: serotonin 5HT_{2B} and H₃ receptors fused to, respectively, the

C-terminal and N-terminal hemi-domains of YFP, or cannabinoid CB₁ and D₁ fused to, respectively, the N-terminal and C-terminal hemi-domains of YFP (ESM 1 : Fig. S1). Cells were then transfected with cDNAs encoding for NR1A-Rluc, NR2B, and H₃ and D₁ receptors fused to, respectively, the N-terminal and C-terminal hemi-domains of YFP. Complementation was confirmed by a saturable BRET signal (Fig. 4h), thus demonstrating the formation of a macromolecular complex containing D₁, H₃, and NMDA receptors. The negative control in cells co-expressing CB₁R-Rluc, D₁R-cYFP, and H₃R-nYFP led to a linear non-specific BRET reflecting the inability of the cannabinoid CB₁ receptor to interact with D₁/H₃RHets (Fig. 4h).

Fig. 4

Detection by energy transfer experiments of complexes formed by NR1A and D₁ and H₃ receptors. **a** Scheme of the BRET technique. One receptor (R1) fused to Rluc (BRET donor) and a closely located receptor (R2) fused to YFP (BRET acceptor) allows, prior addition of a Rluc substrate, energy transfer, and fluorescence emission at 530 nm. **b–e** BRET saturation experiments were performed using HEK293 T cells 48 h post-transfection with 0.2 µg of cDNA for NR1A-Rluc with (**c, e**) or without (**b, d**) the same amount of cDNA for NR2B and increasing amounts of cDNA for D₁R-YFP (0.5–4.5 µg cDNA) (**b, c**) or H₃R-YFP (0.5–4.5 µg cDNA) (**d, e**). **f** As in **e** but in cells also transfected with 2 µg of cDNA for D₁ receptors (full human version) and treated with 1 µM of dopamine. **g** Scheme of BRET combined with bimolecular fluorescence complementation (BiFC) to detect D₁R-H₃R-NMDA receptor heteromers. In this assay, the BRET donor consists of Rluc fused to the NR1A NMDA receptor subunit (*orange*). The acceptor for BRET (YFP Venus) is reconstituted if H₃R (*blue*) fused to the N-terminal half of YFP is close to D₁R (*green*) fused to the C-terminal half of YFP Venus. **h** BRET with bimolecular fluorescence complementation (BiFC) experiments were carried out 48 h post-transfection using 0.05 µg of cDNA for NR1A-Rluc and to NR2B (or 0.08 µg of cDNA for CB₁R-Rluc) and increasing amounts of cDNA for H₃R-nYFP (0.5–6 µg cDNA) and D₁R-cYFP (0.5–3 µg cDNA). Both fluorescence and luminescence of each sample were measured in every experiment to confirm similar donor expressions (~130,000 bioluminescence units) while monitoring the increase in acceptor expression (10,000–40,000 fluorescence units in BRET saturation experiments and 10,000–25,000 fluorescence units in BiFC experiments). The relative amount of BRET is

given as a function of $100 \times$ the ratio between the fluorescence of the acceptor (YFP) and donor (Rluc) expression. BRET and BiFC are expressed as milliBRET units (mBU) and values are the mean \pm SEM from four to ten different experiments grouped as a function of the amount of acceptor



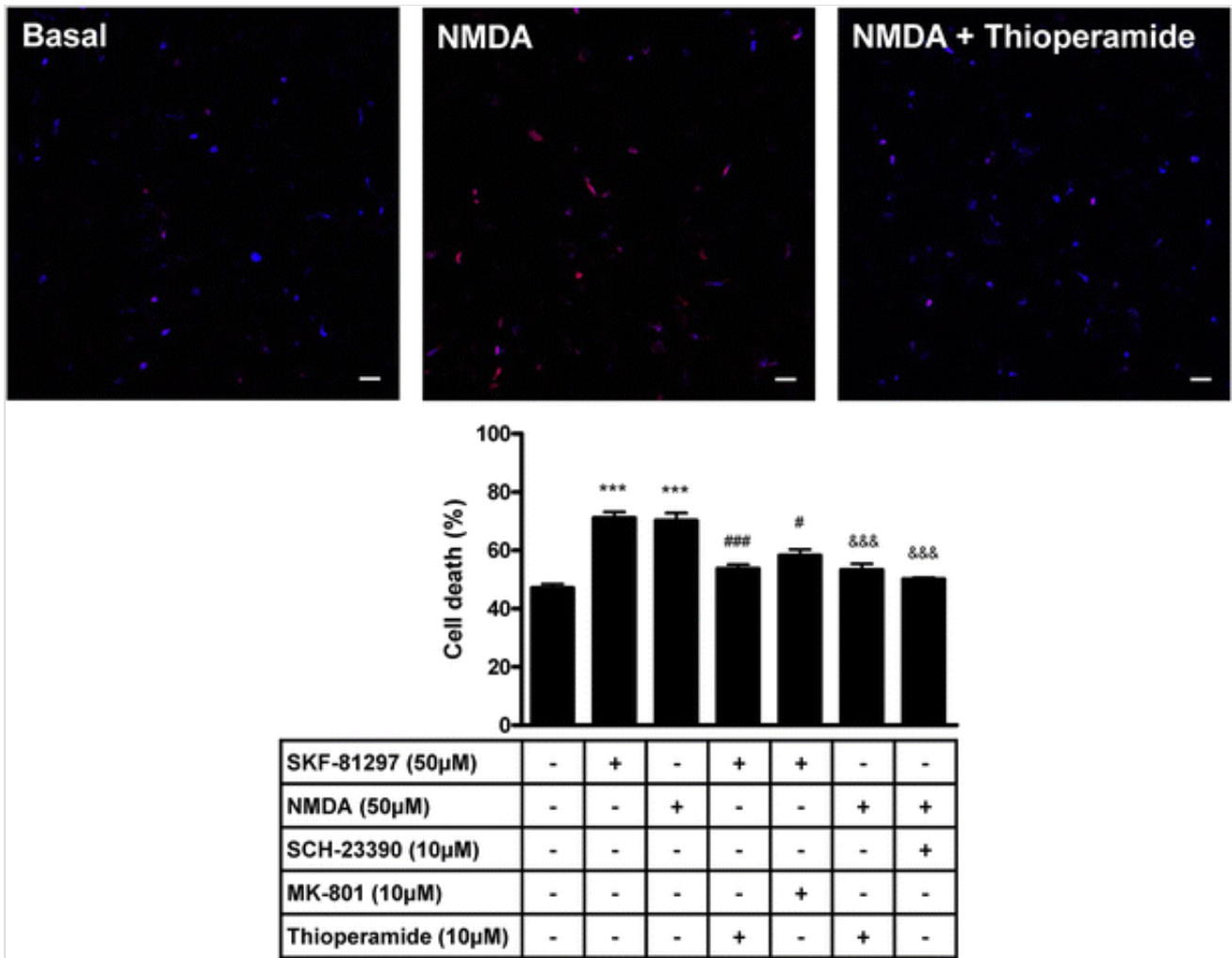
In Vitro Neuroprotection

The effect on NMDA-mediated excitotoxicity of D₁ and H₃ receptor ligands was tested in slices from rat cortex. Images comparing Hoechst and propidium iodide labeling are shown in Fig. 5 (top). Quantification of dead versus total cells showed that NMDA but also SKF-81297, a full D₁ receptor agonist, were able to significantly induce cell death (Fig. 5, bottom). A selective NMDA antagonist, MK-801, partially reversed the SKF-81297-induced toxicity. The D₁ receptor selective antagonist, SCH-23390, and, interestingly, the selective H₃

receptor antagonist, thioperamide, were able to markedly reduce the toxicity induced by NMDA (Fig. 5, bottom).

Fig. 5

Functional interactions between D₁, H₃, and NMDA receptors at the level of excitotoxic cell death in rat brain organotypic cultures. Organotypic cultures of rat cortical slices were prepared as indicated in “Materials and Methods.” Twenty-four hours post-dissection, culture medium was replaced by fresh medium containing vehicle or 10 μM SCH-23390, MK-801, or thioperamide. Slices were incubated for 1 h before the addition of the D₁ receptor agonist SKF-81297 (50 μM) or NMDA (50 μM) and samples were maintained 48 h more in culture. Cell death was determined by comparing Hoechst and propidium iodide (PI) staining as indicated in “Materials and Methods.” *Top*: Representative images of control (basal) and treated (NMDA and NMDA plus thioperamide) samples. *Bottom*: Values represent mean ± SEM of the percentage of PI-stained cells versus total Hoechst-stained cells (the 100 % value would represent all cell death) determined in 10–12 fields from three independent organotypic cultures. Scale bars: 20 μm. One-way ANOVA followed by Bonferroni’s post hoc test showed a significant effect over vehicle-treated (***p* < 0.001), SKF-81297-treated ([#]*p* < 0.05, ^{###}*p* < 0.001), or NMDA-treated (&&&*p* < 0.001) cultures

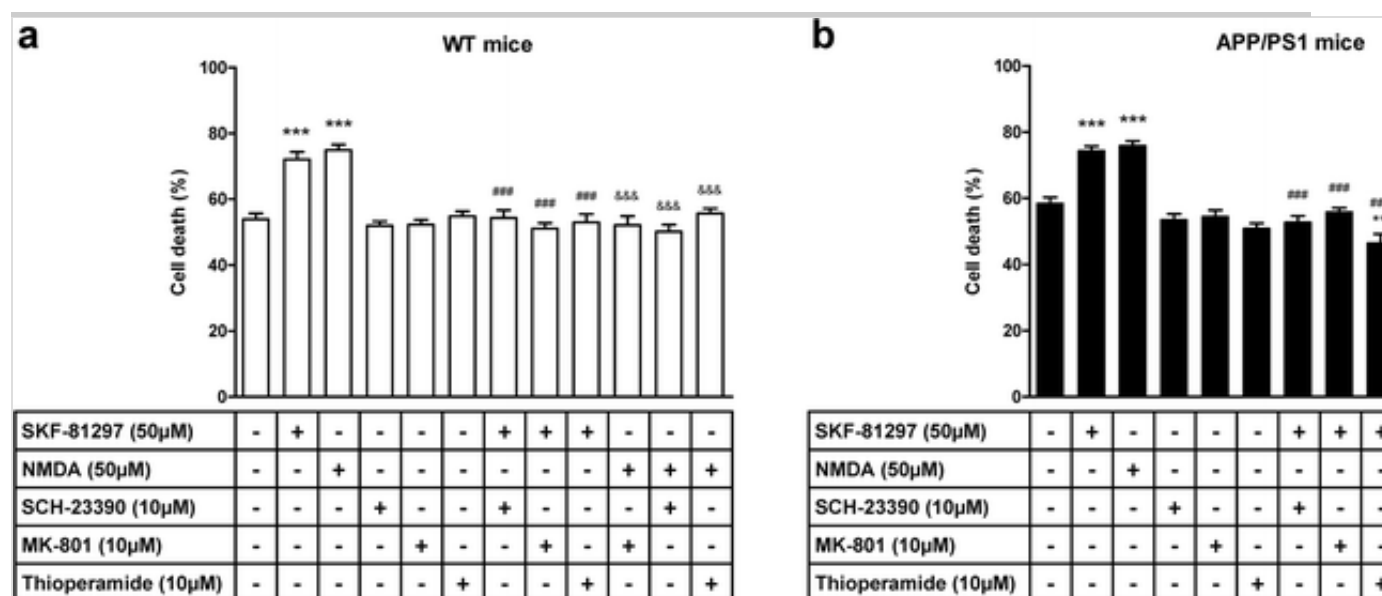


Similar experiments were performed in slices from a transgenic model of Alzheimer's disease, namely the APP/PS1 mouse. Brain cortical slices from APP/PS1 and age-matched non-transgenic (wild-type) animals were treated with NMDA or SKF-81297 to provoke excitotoxic neuronal cell death. The two drugs led to a significant cell death in samples from the two animal groups that was prevented by 10 μM MK-810, the selective NMDA receptor antagonist. The antihistamine drug (10 μM thioperamide) also led to a significant prevention of excitotoxic damage. Neuroprotection was also afforded by thioperamide in samples from APP/PS1 animals treated with SKF-81297. In addition, the D₁ receptor selective antagonist SCH-23390 also counteracted the death induced by NMDA (Fig. 6a, b). Overall, neuroprotection data show the interplay between the three receptors and that antagonists may prevent excitotoxic neuronal death.

Fig. 6

Functional interactions between D₁, H₃, and NMDA receptors at the level of

excitotoxic cell death in organotypic cultures from APP/PS1 and age-matched wild-type mice. Organotypic cultures of cortical slices from wild-type (a) and APP/PS1 (b) mice were prepared as indicated in “Materials and Methods.” Cultures in fresh medium containing vehicle or 10 μ M SCH-23390, MK-801, or thioperamide were then incubated for 1 h before the addition of the D₁ receptor agonist SKF-81297 (50 μ M) or NMDA (50 μ M) and samples were maintained 48 h more in culture. Cell death was determined by Hoechst and propidium iodide (PI) staining as indicated in “Materials and Methods.” Values represent mean \pm SEM of the percentage of PI-stained cells versus total Hoechst-stained cells (the 100 % value would represent all cell death) determined in 10–12 fields from three independent organotypic cultures. One-way ANOVA followed by Bonferroni’s post hoc test showed a significant effect over vehicle-treated ($***p < 0.001$), SKF-81297-treated ($####p < 0.001$), or NMDA-treated ($&&&p < 0.001$) organotypic cultures. Two-way ANOVA showed no significant differences on comparing data from wild-type and APP/PS1 mice



Expression of Heteromers in Cortex from APP/PS1 Mice

Unfortunately, there is not any reliable methodology to detect three interacting proteins in natural sources. Thus, the potential expression of macromolecular complexes in cortex was addressed by PLA assays aimed at detecting heteromers between pairs of proteins. Using combinations of antibodies, macromolecular complex expression was assayed in the cortex of wild-type and APP/PS1 mice, which exhibits an accelerated AD phenotype due to

overexpression of the human amyloid precursor protein harboring the *Swedish* double mutation and of the presenilin-1 L166P mutant. Red dots reflecting positive PLA were observed in samples treated with antibodies against D₁ and H₃ receptors, with antibodies against D₁ and NR1A receptors and with antibodies against H₃ and NR1A. The number of red dots after PLA was negligible in the negative controls, obtained by doing the PLA experiments in wild-type and APP/PS1 mice brain sections only incubated with antibodies against D₁ (Fig. 7a, b) or against H₃ receptors (not shown). In cortical sections from wild-type mice, the percentage of cells expressing D₁-H₃, NMDA/NR1A-D₁, or NMDA/NR1A-H₃ complexes was similar; also similar were the dots/cell ratios (Fig. 7b, black bars). Although indirect, these PLA results constitute evidence that the three receptors form a macromolecular complex. The percentage of dimer-expressing cells was also similar in the cortex from the APP/PS1 mouse (Fig. 7b left, red bars) also suggesting the occurrence in the cortex of APP/PS1 animals of complexes formed by the two GPCRs and the NR1A subunit of the NMDA receptor. Differences in the labeling of the three different pair of proteins between wild-type and APP/PS1 animals were statistically significant but small in magnitude (circa 10 %). Thus, it may be assumed that the differences in the expression of complexes formed by the three proteins are low. Looking at red spots/cell ratios, the highest change in transgenic versus wild-type animals is the expression of dimers formed by H₃ receptors and the NR1A subunit. Such increase correlated with a small increase in the ratio of D₁-NR1A pairs and a small increase in the ratio of H₃-NR1A pairs (Fig. 7b, right panel). These results highlight the occurrence in the cortex of the AD mouse of pairs of proteins, and allegedly of complexes of the three receptors, at levels comparable to those found in samples from wild-type animals. Due to the relevance of A β peptide toxicity in Alzheimer's disease pathophysiology, we assayed whether the H₃ receptor antagonist could be neuroprotective against the toxic action of A β . Images comparing Hoechst and propidium iodide labeling are shown in Fig. 8 (top), and the results showed that 10 μ M thioperamide was totally effective in blocking the toxic effect of 1 μ M A β ₁₋₄₂ peptide (Fig. 8, bottom). Similar effects were obtained with other selective H₃ receptor antagonists (not shown). Our results suggest hetero-oligomer formation in cortex from wild-type and APP/PS1 animals and show that antagonists of dopamine or of histamine receptors consistently afford neuroprotection against excitotoxic agents or A β ₁₋₄₂ peptide.

Fig. 7

Detection of D₁-H₃, NR1A-D₁, and NR1A-H₃ receptor complexes in APP/PS1 and age-matched wild-type mice. D₁-H₃, NR1A-D₁, and NR1A-H₃ receptor complexes were visualized by PLA as red spots around blue-colored DAPI-stained nucleus in cortical sections from wild-type (**a**, *top*) and APP/PS1 mice (**a**, *bottom*). As negative control (**a**, *left*), PLA experiments were performed in sections incubated with one primary antibody (against the D₁ receptor). Scale bar: 20 μm. In **b** (*left*), a graph shows the number of cells containing one or more red spots, expressed as a percentage respect the total number of cells (blue nucleus). The graph in the right shows *r* values (number of red spots/cell containing spots). Data are mean ± SEM of counts in 1000–2000 cells from 7–16 different fields from each condition from three different animals. One-way ANOVA followed by Dunnett's post hoc test showed significant differences (***p* < 0.01, ****p* < 0.001) on percentage of positive cells and ratio respect to negative control (D₁). Two-way ANOVA after Bonferroni's post hoc test comparing data from wild-type and APP-PS1 mice showed significant differences (#*p* < 0.05, ##*p* < 0.01, ###*p* < 0.001) in percentage of cells expressing PLA for any protein pair, and in the number of spots/cell for D₁-H₃, (#*p* < 0.05) and NR1A-H₃ (####*p* < 0.001) but not for NR1A-D₁ heteroreceptor complexes

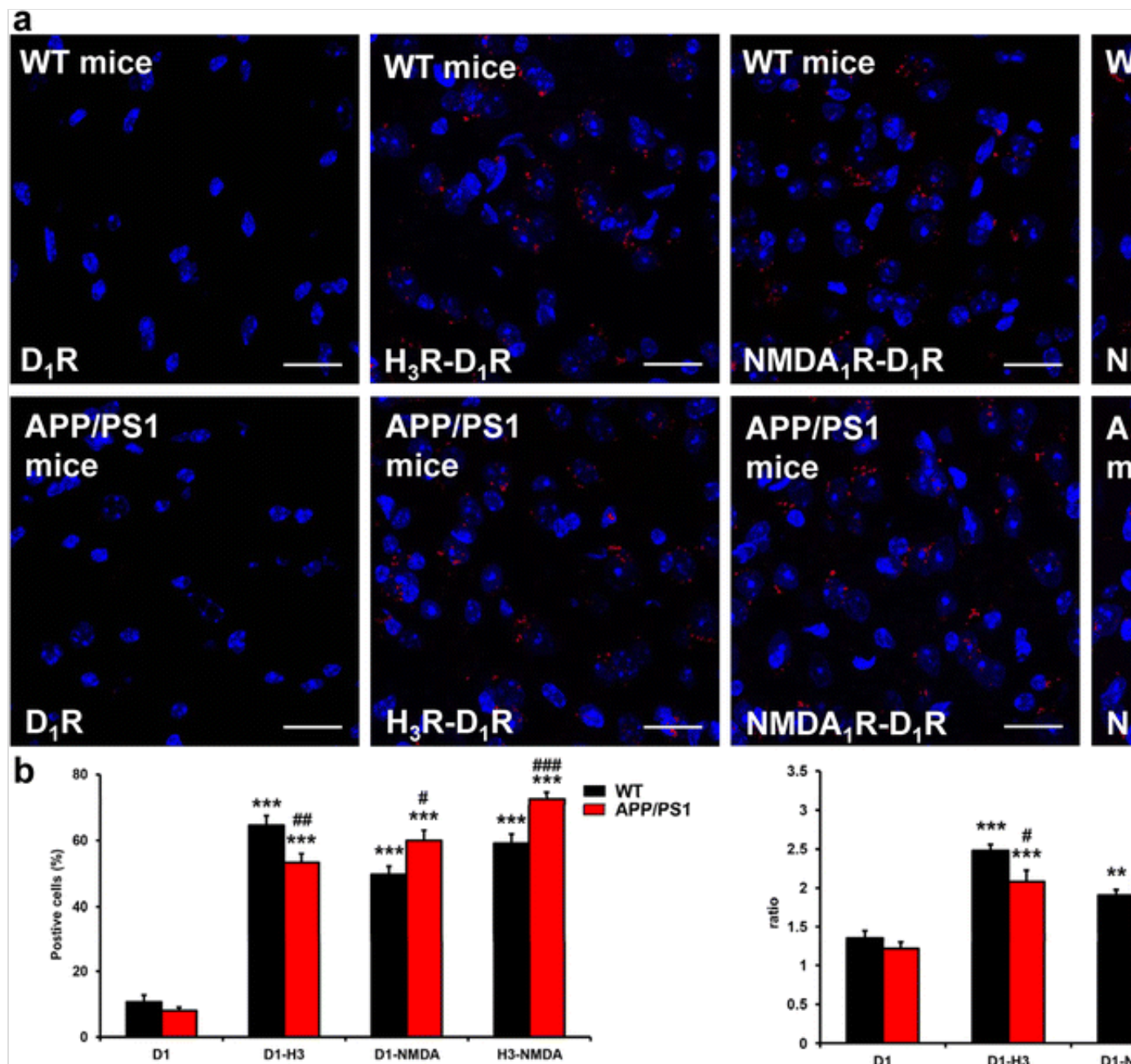
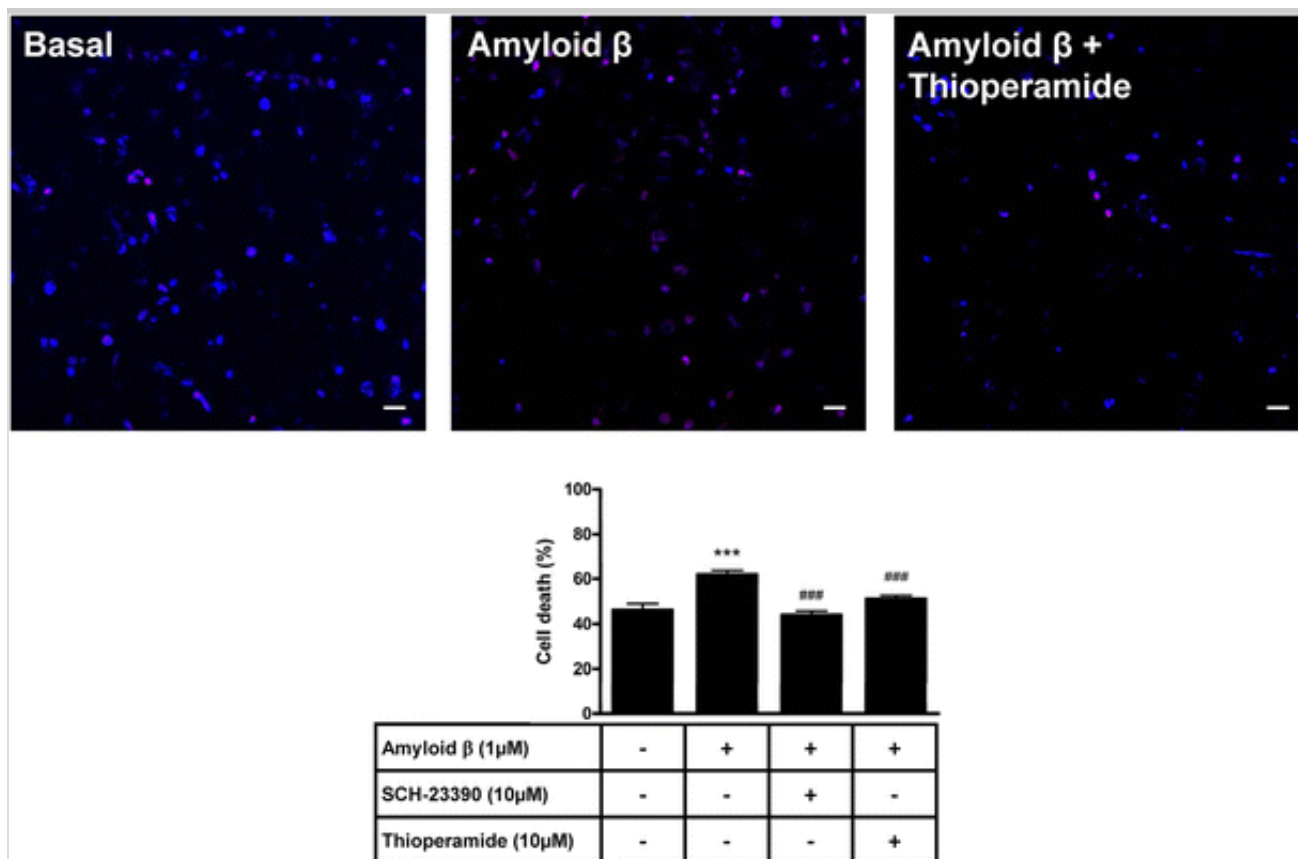


Fig. 8

$A\beta_{1-42}$ peptide-promoted cell death in rat brain organotypic cultures. Organotypic cultures of rat cortical slices were prepared as indicated in “Materials and Methods.” Cultures in fresh medium containing vehicle or 10 μ M of SCH-23390 or thioperamide were incubated for 1 h before the addition of $A\beta_{1-42}$ peptide (1 μ M) and samples were maintained 48 h more in culture. *Top*: Representative images of control (basal), and treated ($A\beta_{1-42}$ peptide and $A\beta_{1-42}$ peptide plus thioperamide) samples. *Bottom*: Cell death was determined by Hoechst and propidium iodide (PI) staining as indicated in “Materials and Methods.” Values represent mean \pm SEM of the percentage of PI-stained cells versus total Hoechst-

stained cells (the 100 % value would represent all cell death) determined in 10–12 fields from three independent organotypic cultures. One-way ANOVA followed by Bonferroni's post hoc test showed a significant effect over vehicle-treated ($***p < 0.001$) or $A\beta_{1-42}$ peptide-treated ($####p < 0.001$) organotypic cultures. Scale bars: 20 μm



Discussion

Dopamine and NMDA receptor interactions have potential from a therapeutic point of view. A main issue on targeting post-synaptic receptors with agonist or antagonists is the alteration of important neural functions (reviewed in [25]). Activation of D_1 and NMDA receptors converge in the ERK1/2 MAP kinase cascade [33]. pERKs translocate to the nucleus and engage transcription factors involved in neural plasticity and survival or death mechanisms.

Neural cell toxicity by dopamine is mediated by both cell surface receptors [34, 35] and by intracellular metabolism leading to increased $\text{NAD(P)}^+/\text{NAD(P)H}$ ratios (Giménez-Xavier et al. 2006 and references therein) [37]. Reported a dopamine-induced increase in cytosolic SULT1A1/3 sulfotransferase levels, the

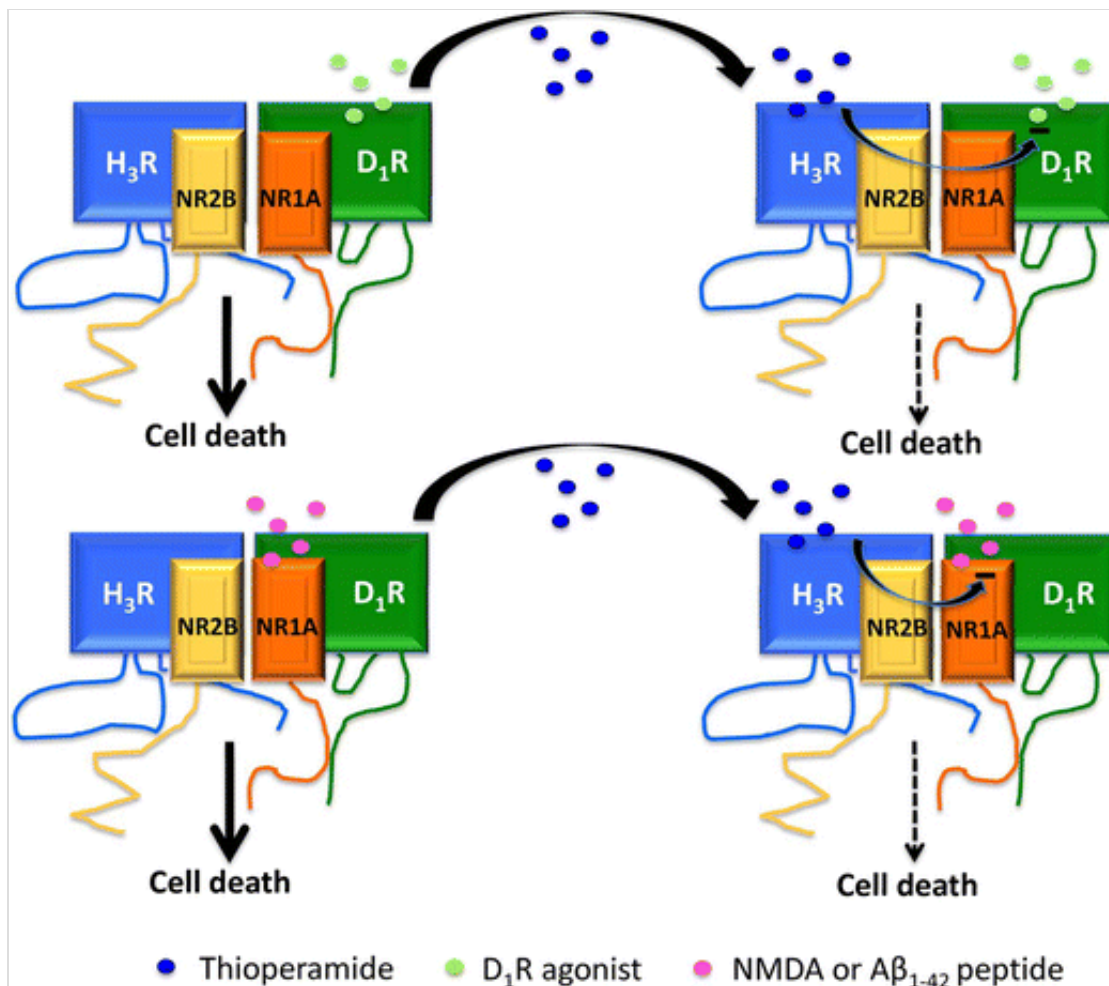
enzyme that metabolizes the neurotransmitter to dopamine-sulfate. Induction of sulfotransferases is preceded by dopamine-receptor-mediated ERK phosphorylation and inhibited by the D₁ receptor antagonist SCH-23390. Interestingly, induction of SULT1A1/3 requires NMDA receptor signaling thus suggesting a dopamine D₁-NMDA receptor-mediated mechanism [37].

The quaternary structure of receptor complexes is a key for signaling to the MAP kinase cascade [38]. The NR1A and NR2A subunits of the NMDA receptor interact with two regions in the carboxyl tail of the D₁ receptor. Interestingly, one interaction is involved in modulating receptor-gated currents and the other in the attenuation of NMDA receptor-mediated excitotoxicity [24]. Our results suggest the formation of heteromers formed by D₁, H₃, and NR1A-NR2B NMDA receptors in which the quaternary structure of the complex allows close contacts between D₁ and H₃ receptors and the two NMDA receptor subunits. PLA studies in cortical sections from rats and mice, including the APP/PS1 transgenic line, showed aggregates formed by NMDA, D₁ and/or H₃ receptors that are suggestive of complexes formed by the three receptors. Indeed, in vitro assays using BRET and bimolecular fluorescence complementation constitute evidence of complexes containing D₁, H₃, and NR1A-NR2B NMDA receptors. Dopamine-induced increase of BRET_{max} between NR1A-Rluc and H₃-YFP (in the presence of the NR2B subunit and the D₁ receptor) reflects the allosteric interactions expected when one receptor within the hetero-oligomer is activated. Alteration of the quaternary structure of the overall macromolecular complex by H₃ receptor antagonists seems to uncouple the death program induced by engagement of D₁ or NMDA receptors (Fig. 9). The protection afforded in rat cortical slices by the H₃ receptor antagonist, thioperamide, was virtually complete. It is worth noting that thioperamide in cortical slices from APP/PS1 mice reverted the excitotoxic shock. Although not statistically significant, there was a tendency of thioperamide decreasing the degree of death in APP/PS1 slices incubated with medium lacking any added compound. The neuroprotection exerted by thioperamide in wild-type and APP/PS1 mice was very similar, being this result consistent with the similar level of expression of D₁/H₃, D₁/NR1A, or H₃/NR1A pairs of proteins in the cerebral cortex from both animal groups. Assessment of the degree of expression of complexes formed by the three (D₁, H₃, and NMDA) receptors cannot be direct. Hence, extrapolating the pairwise

PLA results in Fig. 7, it is likely that the differences in percentage of cells or red spots/cell shown would account for a maximum difference of 10 % in the expression of triple complexes in AD versus wild-type mice. Remarkably, the evidence of marked D_1 - H_3 -NMDA receptor complex expression in mice exhibiting an accelerated AD phenotype due to overexpression of the human amyloid precursor protein make these complexes attractive to combat amyloid-related excitotoxic damage. The increased excitotoxic vulnerability by amyloid protein [39] and evidence of $A\beta$ binding to NMDA receptors [5, 40, 41], prompted the assay of $A\beta$ toxicity that was also prevented by thioperamide. Taken together, the results indicate a neuroprotective potential of H_3 receptor antagonists.

Fig. 9

Scheme depicting how complexes formed by NMDA, D_1 , and H_3 modulate excitotoxic or $A\beta$ 1-42 peptide-mediated cell death. Over stimulation D_1 R by the SKF-81297 agonist (*top panels*) induce cell death that can be reverted by H_3 R antagonist thioperamide. Similarly, NMDA binding to its receptor, or $A\beta$ 1-42 peptide, probably by binding to NMDA receptors (*bottom panels*), induce excitotoxic cell death that can be reverted by H_3 R antagonist thioperamide. Neuroprotection seems to involve a cross-antagonism, i.e., thioperamide-counteracting D_1 or NMDA receptor overstimulation



Passaia and Blandina [42] reviewed data suggesting modulation by histamine via H_3 receptors of cholinergic tone in the cortex and hippocampus and proposed the use of thioperamide as a potential pharmacological intervention to enhance cholinergic input in AD. To our knowledge, thioperamide has not been tested in AD animal models. However, recently released results from a 16-week phase II clinical trial in subjects with mild-to-moderate AD [43] show that a monotherapy with GSK239512, a safe and brain-penetrant selective H_3 receptor antagonist, improves episodic but not working memory or executive functions. Although the cognitive effects were virtually absent in these patients, the potential of H_3 receptor antagonists to prevent disease progression may not be underestimated, and our *in vitro* results show that H_3 receptor antagonism is very efficacious in preventing excitotoxicity and $A\beta$ peptide toxicity. What the results suggest is that H_3 receptor antagonists may not be suitable for what they have been tested until now, namely cognitive enhancement, but for neuroprotection, which is seemingly afforded by targeting H_3 - D_1 -NMDA receptor heteroreceptor complexes.

Acknowledgments

AQ3

We would like to thank Prof. Isidre Ferrer and Dr. Ester Aso for kindly providing the APP/PS1 transgenic animals used in this work and Dr. Julie Perroy for kindly providing constructs encoding NMDA receptor subunits and fusion proteins containing NMDA receptor subunits.

Funding None of the authors have received compensation for professional services.

MRR had and has a predoctoral contract from the University of Barcelona. DMD and PJM had postdoctoral contracts from the Spanish Government. EM and GN had and have research fellow contracts from CIBERNED (Instituto Carlos III, Ministry of Health, Spanish Government). AC, JM, CL, EIC, VC, and RF had and have academic positions linked to the University of Barcelona.

Compliance with Ethical Standards

Animal procedures were conducted according to ethical guidelines (European Communities Council Directive 2010/63/EU) and approved by the animal experimentation ethics committee of the Catalan Government (CEEA-DAAM 6419 and CEEA/DMAH 4049 and 5664).

AQ4

Conflict of Interest This work was supported by grants SAF2009-07276 (RF) from Spanish Ministry of Economy and Innovation (MINECO), 2014-SGR-1236 (EIC) from *Generalitat de Catalunya* and 2140610 (EIC) from the *Fundació La Marató de TV3*. Authors declare no conflict of interests.

Electronic Supplementary Material

Below is the link to the electronic supplementary material.

ESM 1

Fig. S1 Bimolecular fluorescence complementation optimization. Different ratios of plasmids encoding fusion proteins constituted by H₃ or D₁ receptors and either half of the YFP were assayed to optimize fluorescence emission after complementation. HEK293T cells were co-transfected with the indicated amounts

of cDNAs and 48 h post-transfection, fluorescence was determined at 530 nm. The optimal combination of cDNAs was obtained using D₁R-cYFP and H₃R-nYFP (a), where the ratio 1.5 µg and 4 µg, respectively, showed the highest percentage of fluorescence emission respect to non-transfected cells. The inverse combination of cDNAs D₁R-nYFP and H₃R-cYFP (b) showed no significant differences compared to non-transfected cells in all the tested ratios. As negative controls, other non-interacting pairs of receptors were assayed: serotonin 5HT_{2B} and H₃ receptors fused to, respectively, the C-terminal and N-terminal hemi-domains of YFP (c), and cannabinoid CB₁ and D₁ fused to, respectively, the N-terminal and C-terminal hemi-domains of YFP (d). . All negative controls showed no significant differences compared to non-transfected cells. Values are means ± SEM of 3–5 different experiments. One-way ANOVA followed by Dunnett's post-hoc test showed significant (* $p < 0.05$, *** $p < 0.001$,) differences compared to non-transfected cells. (TIFF 1241 kb)

References

AQ5

1. Thathiah A, De Strooper B (2011) The role of G protein-coupled receptors in the pathology of Alzheimer's disease. *Nat Rev Neurosci* 12:73–87. doi: 10.1038/nrn2977
2. Borchelt DR, Thinakaran G, Eckman CB et al (1997) Cellular and molecular mechanisms involved in the neurotoxicity of opioid and psychostimulant drugs. *J Neurosci* 1762:10090–10101. doi: 10.1523/JNEUROSCI.4147-13.2014
3. Borchelt DR, Thinakaran G, Eckman CB et al (1996) Familial Alzheimer's disease-linked presenilin 1 variants elevate Abeta1-42/1-40 ratio *in vitro* and *in vivo*. *Neuron* 17:1005–13
4. Jürgensen S, Antonio LL, Mussi GEA et al (2011) Activation of D1/D5 dopamine receptors protects neurons from synapse dysfunction induced by amyloid-beta oligomers. *J Biol Chem* 286:3270–6. doi: 10.1074/jbc.M110.177790

5. Cowburn RF, Wiehager B, Trief E et al (1997) Effects of beta-amyloid-(25–35) peptides on radioligand binding to excitatory amino acid receptors and voltage-dependent calcium channels: evidence for a selective affinity for the glutamate and glycine recognition sites of the NMDA receptor. *Neurochem Res* 22:1437–42
6. Ferrada C, Moreno E, Casadó V et al (2009) Marked changes in signal transduction upon heteromerization of dopamine D1 and histamine H3 receptors. *Br J Pharmacol* 157:64–75. doi: 10.1111/j.1476-5381.2009.00152.x
7. Moreno E, Vaz SH, Cai N-S et al (2011) Dopamine-galanin receptor heteromers modulate cholinergic neurotransmission in the rat ventral hippocampus. *J Neurosci* 31:7412–23. doi: 10.1523/JNEUROSCI.0191-11.2011
8. Hersi AI, Richard JW, Gaudreau P, Quirion R (1995) Local modulation of hippocampal acetylcholine release by dopamine D1 receptors: a combined receptor autoradiography and in vivo dialysis study. *J Neurosci* 15:7150–7
9. Seong HJ, Carter AG (2012) D1 receptor modulation of action potential firing in a subpopulation of layer 5 pyramidal neurons in the prefrontal cortex. *J Neurosci* 32:10516–21. doi: 10.1523/JNEUROSCI.1367-12.2012
10. Mcnamara CG, Tejero-Cantero Á, Trouche S et al (2014) Dopaminergic neurons promote hippocampal reactivation and spatial memory persistence. *Nat Neurosci* 17:1658–60. doi: 10.1038/nn.3843
11. Fernández-Novoa L, Cacabelos R (2001) Histamine function in brain disorders. *Behav Brain Res* 124:213–33
12. Cacabelos R, Yamatodani A, Niigawa H et al (1989) Brain histamine in Alzheimer's disease. *Methods Find Exp Clin Pharmacol* 11:353–60
13. Panula P, Rinne J, Kuokkanen K et al (1998) Neuronal histamine deficit in Alzheimer's disease. *Neuroscience* 82:993–7

14. Mazurkiewicz-Kwilecki IM, Nsonwah S (1989) Changes in the regional brain histamine and histidine levels in postmortem brains of Alzheimer patients. *Can J Physiol Pharmacol* 67:75–8
15. Medhurst AD, Roberts JC, Lee J et al (2009) Characterization of histamine H3 receptors in Alzheimer's disease brain and amyloid over-expressing TASTPM mice. *Br J Pharmacol* 157:130–8. doi: 10.1111/j.1476-5381.2008.00075.x
16. Pillot C, Heron A, Cochois V et al (2002) A detailed mapping of the histamine H(3) receptor and its gene transcripts in rat brain. *Neuroscience* 114:173–93
17. Bitner RS, Markosyan S, Nikkel AL, Brioni JD In-vivo histamine H3 receptor antagonism activates cellular signaling suggestive of symptomatic and disease modifying efficacy in Alzheimer's disease. *Neuropharmacology* 60:460–6. doi: 10.1016/j.neuropharm.2010.10.026
18. Brioni JD, Esbenshade TA, Garrison TR et al (2011) Discovery of histamine H3 antagonists for the treatment of cognitive disorders and Alzheimer's disease. *J Pharmacol Exp Ther* 336:38–46. doi: 10.1124/jpet.110.166876
19. Chazot PL (2010) Therapeutic potential of histamine H3 receptor antagonists in dementias. *Drug News Perspect* 23:99–103. doi: 10.1358/dnp.2010.23.2.1475899
20. Franco R, Martínez-Pinilla E, Lanciego JL, Navarro G (2016) Basic pharmacological and structural evidence for class A G-protein-coupled receptor heteromerization. *Front Pharmacol* In press:76. doi: 10.3389/fphar.2016.00076
21. Borroto-Escuela DO, Romero-Fernandez W, Garriga P et al (2013) G protein-coupled receptor heterodimerization in the brain. *Methods Enzymol* 521:281–294. doi: 10.1016/B978-0-12-391862-8.00015-6
22. Moreno E, Hoffmann H, Gonzalez-Sepúlveda M et al (2011) Dopamine

D1-histamine H3 receptor heteromers provide a selective link to MAPK signaling in GABAergic neurons of the direct striatal pathway. *J Biol Chem* 286:5846–54. doi: 10.1074/jbc.M110.161489

23. Fiorentini C, Gardoni F, Spano P et al (2003) Regulation of dopamine D1 receptor trafficking and desensitization by oligomerization with glutamate N-methyl-D-aspartate receptors. *J Biol Chem* 278:20196–20202. doi: 10.1074/jbc.M213140200

24. Lee FJS, Xue S, Pei L et al (2002) Dual regulation of NMDA receptor functions by direct protein-protein interactions with the dopamine D1 receptor. *Cell* 111:219–30

25. Wang M, Wong AH, Liu F (2012) Interactions between NMDA and dopamine receptors: a potential therapeutic target. *Brain Res* 1476:154–63. doi: 10.1016/j.brainres.2012.03.029

26. Wilkinson D, Wirth Y, Goebel C (2014) Memantine in patients with moderate to severe Alzheimer's disease: meta-analyses using realistic definitions of response. *Dement Geriatr Cogn Disord* 37:71–85. doi: 10.1159/000353801

27. Wang D, Jacobs SA, Tsien JZ (2014) Targeting the NMDA receptor subunit NR2B for treating or preventing age-related memory decline. *Expert Opin Ther Targets* 18:1121–30. doi: 10.1517/14728222.2014.941286

28. Navarro G, Cordoní A, Zelman-Femiak M et al (2016) Quaternary structure of a G-protein-coupled receptor heterotetramer in complex with Gi and Gs. *BMC Biol* 14:26. doi: 10.1186/s12915-016-0247-4

29. Rodrigues RJ, Almeida T, Díaz-Hernández M et al (2016) Presynaptic P2X1-3 and $\alpha 3$ -containing nicotinic receptors assemble into functionally interacting ion channels in the rat hippocampus. *Neuropharmacology* 105:241–257. doi: 10.1016/j.neuropharm.2016.01.022

30. Navarro G, Carriba P, Gandía J et al (2008) Detection of heteromers formed by cannabinoid CB1, dopamine D2, and adenosine A2A G-protein-

coupled receptors by combining bimolecular fluorescence complementation and bioluminescence energy transfer. *ScientificWorldJournal* 8:1088–97. doi: 10.1100/tsw.2008.136

31. Navarro G, Moreno E, Aymerich M, et al. (2010) Direct involvement of sigma-1 receptors in the dopamine D1 receptor-mediated effects of cocaine. *Proc Natl Acad Sci U S A*. doi: 10.1073/pnas.1008911107

32. Navarro G, Moreno E, Bonaventura J et al (2013) Cocaine inhibits dopamine D2 receptor signaling via sigma-1-D2 receptor heteromers. *PLoS One* 8, e61245. doi: 10.1371/journal.pone.0061245

33. Kaphzan H, O’Riordan KJ, Mangan KP et al (2006) NMDA and dopamine converge on the NMDA-receptor to induce ERK activation and synaptic depression in mature hippocampus. *PLoS One* 1, e138. doi: 10.1371/journal.pone.0000138

34. Chen J, Rusnak M, Luedtke RR, Sidhu A (2004) D1 dopamine receptor mediates dopamine-induced cytotoxicity via the ERK signal cascade. *J Biol Chem* 279:39317–30. doi: 10.1074/jbc.M403891200

35. Jeon S-M, Cheon S-M, Bae H-R et al (2010) Selective susceptibility of human dopaminergic neural stem cells to dopamine-induced apoptosis. *Exp Neurobiol* 19:155–64. doi: 10.5607/en.2010.19.3.155

36. Giménez-Xavier P, Gómez-Santos C, Castaño E et al (2006) The decrease of NAD(P)H has a prominent role in dopamine toxicity. *Biochim Biophys Acta* 1762:564–74. doi: 10.1016/j.bbadis.2006.02.003

37. Sidharthan NP, Minchin RF, Butcher NJ (2013) Cytosolic sulfotransferase 1A3 is induced by dopamine and protects neuronal cells from dopamine toxicity: role of D1 receptor-N-methyl-D-aspartate receptor coupling. *J Biol Chem* 288:34364–74. doi: 10.1074/jbc.M113.493239

38. Navarro G, Ferre S, Cordomi A et al (2010) Interactions between intracellular domains as key determinants of the quaternary structure and function of receptor heteromers. *J Biol Chem* 285:27346–27359. doi:

10.1074/jbc.M110.115634

39. Koh JY, Yang LL, Cotman CW (1990) Beta-amyloid protein increases the vulnerability of cultured cortical neurons to excitotoxic damage. *Brain Res* 533:315–20
40. Le WD, Colom LV, Xie WJ et al (1995) Cell death induced by beta-amyloid 1–40 in MES 23.5 hybrid clone: the role of nitric oxide and NMDA-gated channel activation leading to apoptosis. *Brain Res* 686:49–60
41. Wu J, Anwyl R, Rowan MJ (1995) Beta-amyloid selectively augments NMDA receptor-mediated synaptic transmission in rat hippocampus. *Neuroreport* 6:2409–13
42. Passani MB, Blandina P (1998) Cognitive implications for H3 and 5-HT3 receptor modulation of cortical cholinergic function: a parallel story. *Methods Find Exp Clin Pharmacol* 20:725–33
43. Grove RA, Harrington CM, Mahler A et al (2014) A randomized, double-blind, placebo-controlled, 16-week study of the H3 receptor antagonist, GSK239512 as a monotherapy in subjects with mild-to-moderate Alzheimer's disease. *Curr Alzheimer Res* 11:47–58